

THE NEW DUAL-TEXTURE \mathcal{G} DISTRIBUTION FOR SINGLE-LOOK POLSAR DATA

Salman Khan, Raffaella Guida

University of Surrey, Surrey Space Centre, Guildford, Surrey GU2 7XH, U.K.

ABSTRACT

A new form of \mathcal{G} distribution, called the dual-texture \mathcal{G} distribution, is proposed for Single-Look Complex (SLC) PolSAR data. Unlike the scalar texture product model, the dual texture \mathcal{G} distribution is derived considering different texture variables for co-pol and cross-pol (x-pol) channels. The co-pol and x-pol texture variables are modelled by the Generalized Inverse Gaussian (GIG) distribution, separately. The result is a more flexible multivariate distribution. Also Mellin Kind Statistics (MKS) are utilized to analyze GIG textures, observe evidence of dual texture and to estimate shape parameters.

Index Terms— radar polarimetry, polarimetric synthetic aperture radar, data models

1. INTRODUCTION

For some applications where High Resolution (HR) SAR images are required, single-look processing of SAR images can be of use. SAR images are inherently probabilistic in nature because of the speckle phenomenon. Therefore, understanding their statistical properties is fundamental for accurate segmentation, classification and feature extraction.

It is widely accepted in literature that SLC SAR images follow Gaussian statistics under certain assumptions [1]. However, the Gaussian assumption is not always true, partly due to an increase in sensor resolution. As a result non-Gaussian statistical models have been proposed in literature which provide a more accurate modeling of the HR SAR data.

SAR images have been successfully analyzed using the product model, which states that the observed speckle is the product of a Gaussian distributed speckle noise vector Y_p and the square root of a positive random texture variable t [2]. For a monostatic SAR, Y_p is a 3-dimensional vector, and the observed vector can be represented as:

$$Z_p = [S_{hh} \quad \sqrt{2}S_{hv} \quad S_{vv}]^T \quad (1)$$

where S_{hh} , S_{hv} , and S_{vv} are the complex polarimetric channels. In terms of the product model the p -dimensional com-

plex observation can be written as:

$$Z_p = \sqrt{t}Y_p \quad (2)$$

This model assumes that all polarimetric channels exhibit the same texture, which is a weak assumption as it has been observed that in certain image areas the co-pol channels show different texture than the cross-pol ones [3]. Therefore, for more accurate modeling the possibility of multi-texture modelling of SLC data could be considered as previously done for Multilook (MLK) data [3]. This results in the multi-texture product model. For 3-dimensional SAR data it can be written as [3]:

$$\begin{aligned} Z_p &= [\sqrt{t_{hh}}y_{hh} \quad \sqrt{2t_{hv}}y_{hv} \quad \sqrt{t_{vv}}y_{vv}]^T \\ &= \begin{bmatrix} \sqrt{t_{hh}} & 0 & 0 \\ 0 & \sqrt{2t_{hv}} & 0 \\ 0 & 0 & \sqrt{t_{vv}} \end{bmatrix} \begin{bmatrix} y_{hh} \\ y_{hv} \\ y_{vv} \end{bmatrix} \\ &= T^{\frac{1}{2}}Y_p \end{aligned} \quad (3)$$

where $T = \text{diag}\{t_{hh}, 2t_{hv}, t_{vv}\}$ is a positive definite diagonal matrix ($T > 0$).

In this paper a simplified form of the multi-texture product model, called the dual-texture product model, is presented in the context of the well known \mathcal{G} distribution [4, 5] for SLC PolSAR data. For this purpose, the co-pol and x-pol texture is modeled by the GIG distribution [4]. The resulting original closed form dual-texture PDFs are also listed. MKS are used to show evidences of dual texture. Preliminary results from a new parameter estimation scheme based on log-cumulants for GIG textures are also shown.

2. MODELING MULTI-TEXTURE SINGLE-LOOK DATA

The marginal distribution $f_{Z_p}(z)$ can be calculated by the well known formula:

$$f_{Z_p}(z) = \int_{T>0} f_{Z_p}(z|T)f_T(T)dT \quad (4)$$

For single-look SAR data, Y_p is zero mean complex Gaussian distributed and the conditional probability $f_{Z_p}(z|T)$ is given by (proof omitted for succinctness):

$$f_{Z_p}(z|T) = \frac{1}{\pi^p |C| |T|} \exp\left(-z^* t T^{-\frac{1}{2}} C^{-1} T^{-\frac{1}{2}} z\right) \quad (5)$$

The authors would like to kindly thank EADS Astrium Ltd. for providing the datasets and also acknowledge Stian Normann Anfinssen from the University of Tromsø for valuable discussions and comments.

where C is a $p \times p$ Hermitian covariance matrix given by $C = \mathbf{E}[Y_p Y_p^{*t}]$, with ' z^{*t} ' representing the transposed complex conjugate of z , while $|\cdot|$ is a symbol for determinant. The density generating function can be found by putting (5) in (4):

$$f_{Z_p}(z) = \int_{T>0} \frac{\text{etr}(-C^{-1}T^{-\frac{1}{2}}ZZ^{*t}T^{-\frac{1}{2}})}{\pi^p |C||T|} f_T(T) dT \quad (6)$$

where ' $\text{etr}(\cdot)$ ' is the exponential trace, and for mathematical convenience $\text{Tr}(C^{-1}T^{-\frac{1}{2}}ZZ^{*t}T^{-\frac{1}{2}}) = Z^{*t}T^{-\frac{1}{2}}C^{-1}T^{-\frac{1}{2}}Z$. For a given distribution of the texture matrix $f_T(T)$, $f_{Z_p}(z)$ can be found if the integral in (6) has a closed form.

2.1. GIG Distributed Texture

The GIG PDF is used here to model the texture random variables. Denoted as $\mathcal{N}^{-1}(\alpha, \omega, \eta)$, the GIG PDF is defined as [6]:

$$f_X(x) = \frac{1}{\eta^\alpha 2 K_\alpha(\omega)} x^{\alpha-1} \exp\left(-\frac{\omega}{2} \left(\frac{\eta}{x} + \frac{x}{\eta}\right)\right), x > 0 \quad (7)$$

where $\alpha \in \mathbb{R}$, ω are the shape parameters, while η is the scale parameter, and K_ν is the modified Bessel function of the second kind and order ν . The parameters of GIG PDF vary as:

$$\begin{cases} \omega \geq 0, \eta > 0 & \text{if } \alpha \neq 0 \\ \omega > 0, \eta > 0 & \text{if } \alpha = 0 \end{cases} \quad (8)$$

GIG PDF has been shown to be a very general model capable of modeling a variety of textures [4, 7]. Figure 1 shows the second and third order log-cumulants (k_3, k_2) of Astrium SAR S-band SLC data. The (k_3, k_2) space provides an effective way of understanding textures in PolSAR data. According to the best of our knowledge, the log-cumulant space spanned by the GIG texture PDF is shown here for the first time. It covers the same log-cumulant space as the Fisher texture with the advantage that its shape parameters are easily translatable to the limiting cases of inverse Gamma and Gamma textures.

3. DUAL-TEXTURE \mathcal{G} DISTRIBUTION UNDER RECIPROcity & REFLECTION SYMMETRY

In [3] two assumptions have been made to simplify the multi-texture density generating function for multi-look PolSAR data:

1. the texture random variables of co-pol channels t_{hh}, t_{vv} are equal (reciprocity),
2. the scattering is reflection symmetric, which implies that the co-pol and cross-pol correlations are zero in the averaged covariance matrix [8] i.e.

$$C = \begin{bmatrix} c_{11} & 0 & c_{13} \\ 0 & c_{22} & 0 \\ c_{31} & 0 & c_{33} \end{bmatrix} \quad (9)$$

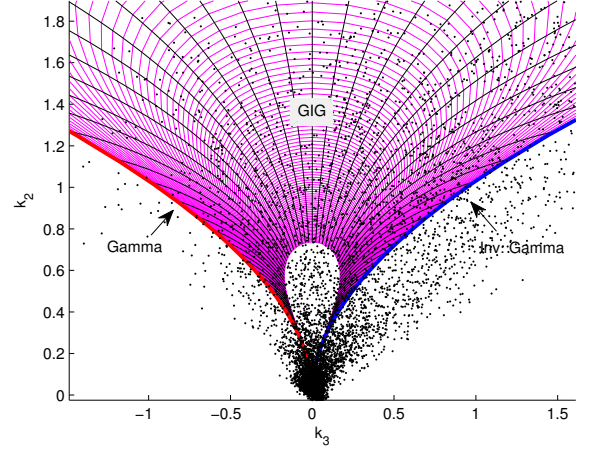


Fig. 1. The (k_3, k_2) log-cumulant space with sample log-cumulants plotted using S-band Astrium demonstrator UK SAR data over Coventry airport. Also depicts the natural position of the GIG texture PDF in the realm of PolSAR statistical modeling.

where c_{ij} denotes the (i, j) th entry of the covariance matrix.

We have used these assumptions in our multi-texture modeling of SLC PolSAR data enabling us to arrive at close form solutions.

3.1. Dual-texture Single-look \mathcal{G} Distribution

An implication of reciprocity and reflection symmetry is that the conditional probability in (5) simply becomes:

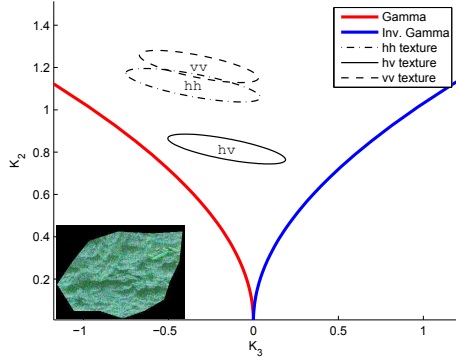
$$f_{Z_p}(z|T) = \frac{1}{\pi^p |C| t_{hh}^2 t_{hv}} \exp\left\{-\left(\frac{q}{t_{hh}} + \frac{r}{t_{hv}}\right)\right\} \quad (10)$$

where $q = z_{11}c_{11} + z_{13}c_{31} + z_{31}c_{13} + z_{33}c_{33}$, $r = z_{22}c_{22}$ and z_{ij} , c_{ij} are the (i, j) th elements of the matrices ZZ^{*t} , C^{-1} respectively. The marginal distribution of the target vector, $f_{Z_p}(z)$, can now be determined under the assumptions of monostatic radar geometry, reciprocity and reflection symmetry:

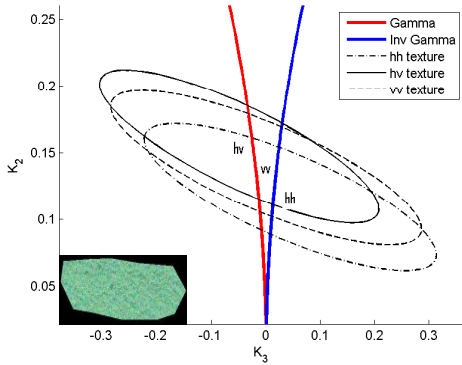
$$f_{Z_p}(z) = \frac{1}{\pi^p |C|} \int_0^\infty \exp\left(-\frac{q}{t_{hh}}\right) \frac{f_{t_{hh}}(t_{hh})}{t_{hh}^2} dt_{hh} \times \int_0^\infty \exp\left(-\frac{r}{t_{hv}}\right) \frac{f_{t_{hv}}(t_{hv})}{t_{hv}} dt_{hv} \quad (11)$$

The GIG PDF in (7) can now be used to model both the co-pol and x-pol texture random variables in (11), resulting in the following expression:

$$f_{Z_p}(z) = \frac{1}{\pi^p |C|} \prod_{i=1}^2 \frac{\lambda_i^{\frac{p-i}{2}} (\gamma_i + s_i)^{\frac{\alpha-p+i}{2}}}{\gamma_i^{\alpha_i/2} K_{\alpha_i}(2\sqrt{\lambda_i \gamma_i})} \times K_{\alpha_i-p+i}(2\sqrt{\lambda_i(\gamma_i + s_i)}) \quad (12)$$



(a) Slight evidence of dual texture over homogeneous trees.



(b) Evidence of scalar texture over homogeneous vegetation.

Fig. 2. The (k_3, k_2) log-cumulant diagram with sample log-cumulants plotted using (a) X-band, (b) S-band Astrium demonstrator UK SAR data over Coventry airport.

where $\lambda_i = \omega_i/\eta_i$, $\gamma_i = \lambda_i^2 \eta_i$, $i = 1, 2$ corresponds to co-pol (co) and x-pol (x) PDFs, respectively, and $s_1 = q$, $s_2 = r$. This distribution, denoted by $\mathcal{G}d_p(\alpha_1, \omega_1, \eta_1, \alpha_2, \omega_2, \eta_2)$, is the dual-texture \mathcal{G} distribution for SLC data and will here on be referred to as simply $\mathcal{G}d_p$. It is the dual-texture counterpart of scalar texture \mathcal{G}_p distribution for SLC data presented in [5].

Just as shown in [4, 5], two special cases of $\mathcal{G}d_p$ can be readily derived using the same Bessel function properties as utilized in [4, 5]. In the first case $\lambda_{1,2} \rightarrow 0^+$, while $\gamma_{1,2} > 0$ and $\alpha_{1,2} < 0$ resulting in dual-texture \mathcal{G}_p^0 PDF ($\mathcal{G}d_p^0$). In the second case $\gamma_{1,2} \rightarrow 0^+$, while $\lambda_{1,2} > 0$ and $\alpha_{1,2} > 0$ resulting in dual-texture \mathcal{K}_p PDF ($\mathcal{K}d_p$). Closed forms of $\mathcal{G}d_p^0$ and $\mathcal{K}d_p$ PDFs have not been included in this contribution.

It is worth mentioning that in the context of log-cumulant diagram of fig. 1, the $\mathcal{G}d_p^0$ and $\mathcal{K}d_p$ PDFs can assume different co- and x-pol textures along the blue and red lines, respectively. In contrast to this, the $\mathcal{G}d_p$ can assume different co- and x-pol textures in the whole space between these limiting cases.

4. ISOLATING TEXTURE IN SLC POLSAR DATA

Texture variables in PolSAR data are not directly observable, but their contribution to the log-cumulants can be measured by subtracting out the theoretical speckle contribution. Then, the texture log-cumulants can be examined in the (k_3, k_2) log-cumulant space as the second and higher order log-cumulants are independent of the scale. Univariate MKS were first applied to radar data by J.-M. Nicolas in his paper, which has been translated in english [9]. The theoretical formulation for such an analysis on SLC and MLK PolSAR data was presented in [10] and [3], respectively. We will only examine SLC univariate texture isolation in this paper as the dual- and scalar-texture isolation is still under analysis. Here we list only the required relations from the detailed theory in [10]. The starting point here is the Fixed Point-Polarimetric Whitening Filter (FP-PWF):

$$\begin{aligned} w &= Z_p^{*t} \hat{\Sigma}_{\text{FP}}^{-1} Z_p \\ &= t(y_p^{*t} \hat{\Sigma}_{\text{FP}}^{-1} y_p) = tQ \end{aligned} \quad (13)$$

The texture (t) PDF is chosen at will so its log-cumulants depend on the chosen PDF. The quadratic form Q has been shown to be a Fisher-variate with its 2nd and higher order log-cumulants given by [10]:

$$k_{v>1}\{Q\} = \psi^{(v-1)}(p) - \psi^{(v-1)}\left(\frac{p(n-p+\frac{1}{p})}{p+1}\right) \quad (14)$$

This provides the fundamental concepts for isolating texture in SLC PolSAR data. By applying the relations of MKS to the product model in (13), one readily finds that

$$\begin{aligned} k_v\{w\} &= k_v\{t\} + k_v\{Q\} \\ k_v\{t\} &= k_v\{w\} - k_v\{Q\} \end{aligned} \quad (15)$$

The above equation shows that the texture log-cumulants can be calculated by removing the speckle contribution ($k_v\{Q\}$) from the polarimetric whitened observation ($k_v\{w\}$). It must be pointed out that as long as the texture log-cumulants have closed forms, we only need to use as many log-cumulant equations (of different orders) as the number of unknown texture parameters for shape parameter estimation. The scale parameter still needs to be estimated separately.

Using the above analysis one can isolate texture occurring in homogeneous areas of SLC PolSAR images to see evidence of scalar-, dual- or multi-texture. A hypothesis testing scheme was developed in [3] to assess the existence of scalar-, dual- or multi-texture for MLK data. Such a scheme for SLC data is beyond the scope of this contribution, however, univariate texture isolation has been performed for SLC data. Two examples depicting scalar and dual textures are shown here.

Figure 2 shows texture log-cumulants plotted in the (k_3, k_2) log-cumulant space. The 95% confidence level ellipses of the (k_3, k_2) points are also shown. No vh points have

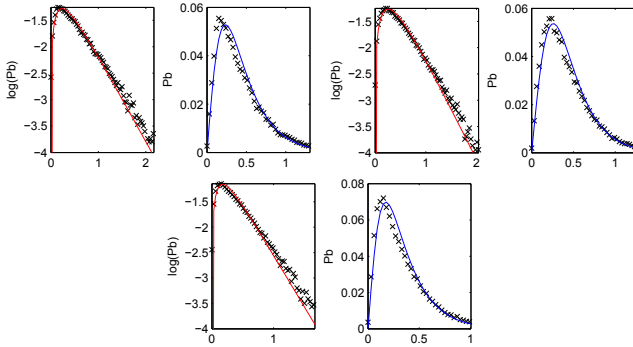


Fig. 3. Fitting of univariate \mathcal{G} PDF to hh (left top pair), hv (right top pair) and (vv) (bottom pair) amplitudes.

been shown because the radar had monostatic geometry. Figure 2 (a) shows these ellipses for a homogeneous trees area. These texture cumulants show slight evidence of dual texture. Other evidences of dual-texture have also been observed. Figure 2 (b) shows evidence of scalar texture variable for a homogeneous vegetation area. The $\mathcal{G}d_p$ PDF can therefore be a useful tool with its co- and x-pol texture variables.

5. PARAMETER ESTIMATION

The shape parameters of the $\mathcal{G}d_p$ distribution for co-pol and x-pol texture variables can be readily estimated from the univariate parameter estimates. This procedure requires averaging the (k_3, k_2) log cumulants of the co-pol and x-pol channels separately and then using them to estimate the shape parameters of $\mathcal{G}d_p$, which is a simple 'plug and play' procedure. The intriguing concept is the shape parameters estimation of GIG textures as it does not have closed form log-cumulant equations. It is sufficient to state here that a new method for fast and accurate shape parameter estimation of the GIG textures has been devised, which is based on using a detailed look-up table of (k_3, k_2) log cumulants, which is in turn used to invert the shape parameters.

Figure 3 shows the univariate amplitude fittings to the \mathcal{G} distribution in both log and linear scale for the X-band data from fig. 2 (a). The log scale is used to emphasize the fitting of the tails of the distributions. It is clear from the figure that the fittings are 'fairly' accurate considering the fact that the estimation is very fast (estimation for 0.1 million pixels takes less than 2 seconds).

6. CONCLUSIONS AND FUTURE WORK

In this paper the new dual-texture single-look $\mathcal{G}d_p$ distribution has been proposed. The $\mathcal{G}d_p$ results when the co-pol and x-pol textures are separately modeled by GIG distribution and the assumptions of reciprocity and reflection symmetry are

applied. It has also been found out that although many homogeneous areas exhibit scalar texture, the dual-texture assumption is also often valid. The GIG texture modeling offers as much flexibility in modeling texture as the Fisher PDF. Some preliminary results of a new log-cumulant based parameter estimation method have been shown for univariate \mathcal{G} distribution and are easily usable in $\mathcal{G}d_p$ PDF. This contribution aims towards better image classification, segmentation and feature extraction. Further work is underway to isolate texture for dual and scalar texture cases of SLC MKS.

7. REFERENCES

- [1] J.-S. Lee and E. Pottier, *Polarimetric Radar Imaging: From Basics to Applications*, chapter 4, pp. 101–107, CRC Press, 2009.
- [2] C. Oliver and S. Quegan, *Understanding Synthetic Aperture Radar Images*, chapter 5, pp. 130–135, SciTech Publishing, 2004.
- [3] T. Eltoft, S.N. Anfinson, and A.P. Doulgeris, "A multi-texture model for multilook polarimetric radar data," in *Geoscience and Remote Sensing Symposium (IGARSS), 2011 IEEE International*, July 2011, pp. 1048–1051.
- [4] C.C. Freitas, A.C. Frery, and A.H. Correia, "The polarimetric \mathcal{G} distribution for SAR data analysis," *Environmetrics*, vol. 16, no. 1, pp. 13–31, 2005.
- [5] S. Khan and R. Guida, "The new form of \mathcal{G} distribution for single-look PolSAR data," in *9th European Conference on Synthetic Aperture Radar '12, to appear*, 2012.
- [6] Chao-Wei Chou and Wen-Jang Huang, "On characterizations of the gamma and generalized inverse gaussian distributions," *Statistics & Probability Letters*, vol. 69, no. 4, pp. 381–388, 2004.
- [7] S. Khan and R. Guida, "On single-look multivariate \mathcal{G} distribution for PolSAR data," *IEEE J. Sel. Top. App. Earth Obs. Remote Sens.*, 2012.
- [8] T. L. Ainsworth, M. Preiss, N. Stacy, M. Nord, and J.-S. Lee, "Analysis of compact polarimetric SAR imaging modes," in *3rd International Workshop on Science and Applications of SAR Polarimetry and Polarimetric Interferometry '07*, January 2007.
- [9] S.N. Anfinson, *Statistical analysis of multilook polarimetric radar images with Mellin transform.*, Ph.D. thesis, University of Tromsø, Tromsø, May 2010.
- [10] S. Anfinson, "On the supremacy of logging," in *Proc. PolInSAR, Frascati, Italy*, 2011.